CSIRO PUBLISHING

International Journal of Wildland Fire **2019**, *28*, 230–236
https://doi.org/10.1071/WF18164

Research Note

Inferring energy incident on sensors in low-intensity surface fires from remotely sensed radiation and using it to predict tree stem injury

Matthew B. Dickinson [A,F], *Bret W. Butler* [B], *Andrew T. Hudak* [C], *Benjamin C. Bright* [C], *Robert L. Kremens* [D] *and Carine Klauberg* [E]

[A]USDA Forest Service, Northern Research Station, Forestry Sciences Laboratory, 359 Main Road, Delaware, OH 43015, USA.
[B]USDA Forest Service, Rocky Mountain Research Station, Fire Sciences Laboratory, 5775 US Highway 10 West, Missoula, MT 59801, USA.
[C]USDA Forest Service Rocky Mountain Research Station, Forestry Sciences Laboratory, 1221 South Main Street, Moscow, ID 83843, USA.
[D]Rochester Institute of Technology, Carlson Center for Imaging Science, 54 Lomb Memorial Drive, Rochester, NY 14623, USA.
[E]Federal University of São João Del Rei – UFSJ, Sete Lagoas, Minas Gerais 35701-970, Brazil.
[F]Corresponding author. Email: mbdickinson@fs.fed.us

Abstract. Remotely sensed radiation, attractive for its spatial and temporal coverage, offers a means of inferring energy deposition in fires (e.g. on soils, fuels and tree stems) but coordinated remote and *in situ* (in-flame) measurements are lacking. We relate remotely sensed measurements of fire radiative energy density (FRED) from nadir (overhead) radiometers on towers and the Wildfire Airborne Sensor Program (WASP) infrared camera on a piloted, fixed-wing aircraft to energy incident on *in situ*, horizontally oriented, wide-angle total flux sensors positioned ~0.5 m above ground level. Measurements were obtained in non-forested herbaceous and shrub-dominated sites and in (forested) longleaf pine (*Pinus palustris* Miller) savanna. Using log–log scaling to reveal downward bias, incident energy was positively related to FRED from nadir radiometers ($R^2 = 0.47$) and WASP ($R^2 = 0.50$). As a demonstration of how this result could be used to describe ecological effects, we predict stem injury for turkey oak (*Quercus laevis* Walter), a common tree species at our study site, using incident energy inferred from remotely sensed FRED. On average, larger-diameter stems were expected to be killed in the forested than in the non-forested sites. Though the approach appears promising, challenges remain for remote and *in situ* measurement.

Additional keywords: Eglin Air Force Base, fire behaviour, fire effects, fire radiated energy, longleaf pine, *Pinus palustris*, *Quercus laevis*, RxCADRE project, tree mortality, turkey oak, Wildfire Airborne Sensor Program (WASP).

Received 12 March 2018, accepted 5 December 2018, published online 14 March 2019

Introduction

Airborne, space-borne and near-ground sensors with nadir (overhead) perspective have shown promise for spatially quantifying fireline progression (Paugam *et al.* 2013), fire intensity (Kremens *et al.* 2012; Johnston *et al.* 2017), area burned (Giglio *et al.* 2006), biomass consumption (Wooster *et al.* 2003, 2005), emissions production (Ichoku and Kaufman 2005) and post-fire effects (Lentile *et al.* 2006; Kremens *et al.* 2010). Energy production, transfer and deposition on fuels drive wildland fire ignition, rate of spread (ROS) and intensity (Anderson 1969; Yedinak *et al.* 2006; Anderson *et al.* 2010), while first-order fire effects are determined by heat deposition on plants and soils (Butler and Dickinson 2010). However, even basic understanding of energy transfer in wildland flames is limited (Sacadura 2005; Viskanta 2008; Finney *et al.* 2010; Finney *et al.* 2015), likely owing to complex logistics associated with sensor deployment, measurement uncertainty, the high-temperature environment and high-frequency temporal variability (Freeborn *et al.* 2008; Hiers *et al.* 2009; Frankman *et al.* 2013). At the same time, the accuracy of remotely sensed data remains uncertain (Schroeder *et al.* 2014; Kremens and Dickinson 2015; Dickinson *et al.* 2016).

Advancing understanding of energy transfer and deposition in wildland fires, based generally on *in situ* (in-flame) measurements and modelling, in concert with the continued development of active-fire remote sensing, promises a stronger foundation for describing wildland fire behaviour and predicting effects (Butler and Dickinson 2010; Kremens *et al.* 2010).

Table 1. Averaged characteristics of fires in non-forested and forested burn blocks from the RxCADRE 2012 fires

Surface fuels were dominated by a herbaceous and shrub mix in non-forested blocks, and a mix of litter, herbaceous and shrub vegetation and woody material in the pine savanna (forested block). Fuel consumption (*W*) and fireline intensity (*I*) are inferred from nadir radiometer measurements using equations in Kremens et al. (2012, see details on fireline intensity in supplementary material) while whole-block estimates of consumption from Hudak *et al.* (2016b) are included for comparison. Estimates of flame length and depth and fire rate of spread are from video analysis that is not currently available for all blocks (see Butler *et al.* 2016). Sample sizes and standard deviations are provided where relevant (in parentheses)

Fire	Fuel	Date	Nadir radiometers	Hudak *et al.* (2016*b*)				
			I (kW m^{-1})	W (Mg ha^{-1})	W (Mg ha^{-1})	Flame height (m)	Flame depth (m)	Spread rate (m s^{-1})
L2F	Forested	11-Nov-2012	907 (9, 670)	5.0 (9, 2.6)	6.36	0.9 (5, 0.5)	1.3 (5, 0.7)	0.04 (2, 0.05)
L1G	Non-forested	4-Nov-2012	529 (9, 316)	1.3 (9, 0.5)	1.54	0.7 (6, 0.5)	1.1 (5, 0.8)	0.24 (4, 0.30)
L2G	Non-forested	10-Nov-2012	739 (12, 358)	1.5 (12, 0.6)	3.09	0.5 (9, 0.2)	0.8 (9, 0.4)	0.89 (3, 0.38)
S3	Non-forested	1-Nov-2012	479 (5, 79)	1.7 (5, 0.2)	2.56			
S4	Non-forested	1-Nov-2012	234 (4, 172)	1.6 (4, 0.7)	2.04			
S5	Non-forested	1-Nov-2012	564 (5, 269)	2.2 (5, 0.6)	2.19	0.4 (4, 0)	0.8 (4, 03)	0.36 (2, 0.28)
S7	Non-forested	7-Nov-2012	1179 (4, 641)	3.3 (4, 1.8)	1.80			
S8	Non-forested	7-Nov-2012	512 (4, 318)	1.9 (4, 0.7)	2.80			
S9	Non-forested	7-Nov-2012	861 (5, 115)	1.8 (5, 0.9)	1.40			

Efforts continue to develop more physically based fire effects models that promise to be more generally applicable than statistical models (Dickinson and Ryan 2010; Chatziefstratiou *et al.* 2013; Massman 2015). These models generally require measured or modelled heat deposition from fires but options are limited by which heat deposition can be inferred from measured or modelled fire characteristics (Butler and Dickinson 2010). We explore how well energy incident on *in situ* (in-flame) sensors can be inferred from ground-leaving fire radiated energy density (kJ m^{-2}, FRED) measured from nadir (overhead) tower-based radiometers and an airborne longwave infrared sensor during spreading experimental fires in south-eastern US fuels. In turn, we demonstrate how inferred energy deposition can be used to predict tree stem injury, an important ecological effect, for a common south-eastern tree species.

Methods

Data were collected in early November 2012 within an 8 × 4-km area of Eglin Air Force Base in north-western Florida during the Prescribed Fire Combustion and Atmospheric Dynamics Research Experiment (RxCADRE), a coordinated measurements campaign described in Ottmar *et al.* (2016*a*) and associated papers. Nadir radiometer (Dickinson and Kremens 2015) and airborne (Hudak *et al.* 2016*a*) data used here are available on the USDA Forest Service Research Data Archive (https://doi.org/10.2737/RDS-2016-0007, accessed 29 January 2019). Burn blocks were characterised by either a herbaceous and shrub fuel mix maintained as open range through mowing, fire and herbicide application (hereafter termed non-forested), or fire-maintained pine savanna with fuel beds including needle cast, turkey oak litter, herbaceous and shrub vegetation, and woody material (hereafter termed forested). Non-forested blocks included large (L1G and L2G) and small (S3, S4, S5, S7, S8, and S9) burn blocks while there was a single large forested block (L2F). Burn blocks, fuels and fire behaviour are described in Hudak *et al.* (2016*b*), Ottmar *et al.* (2016*b*) and Butler *et al.* (2016) and are summarised in Table 1.

Measurements from two *in situ* instruments (incident flux sensors and cameras) and two remote radiation sensors (tower-mounted and airborne) are considered in the present study. *In situ* measurements were made with a horizontally viewing, wide-angle, incident total flux sensor housed with electronics in a fire-hardened container placed on a tripod 0.5 m above ground level (agl) and typically viewed from a perpendicular perspective by a visible video camera housed in a separate container (Butler *et al.* 2010; Butler *et al.* 2016). The incident total flux sensor is one of two sensors in MedTherm Corporation's uncooled dual-sensor. The other is a radiant flux sensor, the data from which are not used in the present study. The incident total flux sensor (hereafter the incident flux sensor) has near-hemispherical sensitivity to fire radiation incident on a black high-emissivity surface over a thermopile detector contained within a copper plug. The sensor surface is also heated by convection. Raw voltages were recorded at 10 Hz and calibrated to incident flux (kW m^{-2}; see Butler and Jimenez 2009; Frankman *et al.* 2013), which was then time-integrated to provide incident energy (kJ m^{-2}) used in the present study. For the 26 datasets for which video analysis is available, 87% showed fire approaching the face of the incident flux sensor from within ±60°, formerly shown to be the acceptance angle within which fire approach angle has no effect on measurements.

Single-pixel dual-band radiometers were placed on towers with a downward (nadir) perspective (Dickinson *et al.* 2016). The nadir radiometers include a mid- (3–5 μm, Dexter Research LWPSiL2) and long-wave (6.5–20 μm, Dexter Research MW) sensors. See further details in Dickinson *et al.* (2016) along with information on data analysis and application provided in Kremens *et al.* (2010, 2012), Cannon *et al.* (2014) and Hudak *et al.* (2016*b*). The nadir radiometers were mounted 5.5 m agl and, at that height, detect radiation from an area of regard of ~23 m^2 (~2.7-m radius) based on their 52° field of view (FOV). Voltage output from each sensor was logged at a 5-s interval.

Fire Radiated Flux Density (FRFD, kW m^{-2}) is the instantaneous, spatial average aerial emission from the fraction of the nadir radiometer area of regard (pixel) that is

radiating above background (also known as the fire fractional area, A_f, which varies from 0 to 1; see supplementary material available online):

$$\mathrm{FRFD} = \varepsilon A_f \sigma T^4 \quad (1)$$

where ε is emissivity (0 to 1), σ is the Stefan–Boltzmann constant and T is effective temperature of the scene determined by blackbody calibration from the ratio of mid- and long-wave infrared (LWIR) signals. The calculation of FRFD from a dual-band nadir radiometer is described in Kremens *et al.* (2010). Peak FRFD was used to estimate fireline intensity (see supplementary material). FRFD was integrated through time (from first rise above background to first fall to background during cooling) to provide FRED (kJ m^{-2}).

The distribution of *in situ* sensors across large and small burn blocks is mapped in Butler *et al.* (2016). A nadir radiometer was co-located with each *in situ* package so that the incident flux sensor faced inward from the margin of the nadir radiometer's area of regard. Given occasional instrument failures, we report data from $n = 7$ co-located measurements in the large forested block and $n = 42$ co-located measurements in non-forested blocks. All ground sensors were geolocated with sub-metre accuracy with a survey-grade global positioning system (GPS).

The Wildfire Airborne Sensor Program (WASP) LWIR camera was flown 1550–3160 m agl on a piloted, fixed-wing aircraft that made repeated passes over the three large burn blocks (see Hudak *et al.* 2016*a*, 2016*b* for data and more detail respectively). The WASP passband is 8–9.2 μm with the spectral response function on file with the Rochester Institute of Technology, Carlson Center for Imaging Science. The WASP camera collected image frames at a 3-s interval as it passed over burn units and there was a 3–4-min gap between the last image frame on a pass and the first frame on the next pass made after turning. Image frames were georectified with *GDAL* based on inertial measurement unit data. Measured voltages, blackbody calibration and a model of radiation from pixels containing a mix of combusting fuels and background were used to calculate FRFD as described in Kremens and Dickinson (2015) and Dickinson *et al.* (2016). Time series for each pixel of radiated flux greater than the background of 1070 W m^{-2} (FRFD) were time integrated as follows:

$$\mathrm{FRFD_{obs}} = \sum_{i=\mathrm{initial}}^{n} 0.5(\mathrm{FRED}_{i+1} + \mathrm{FRED}_i)(t_{i+1} - t_i) \quad (2)$$

where i is image frame number, t is time (s), and the integration is performed from the initial to final (n) frame containing above-background values. A burn-block average correction of resulting $\mathrm{FRED_{obs}}$ maps was applied to account for temporal undersampling and the occasional lack of full coverage of burn blocks by image frames on every pass. Finally, kriging of the resulting FRED estimates where only the pixels with the greatest FRED values (primarily those along flame fronts) were interpolated providing a spatially continuous map of FRED more accurate at the burn block level (see details in Klauberg *et al.* 2018). Average FRED was then calculated for each nadir radiometer (circular) area of regard by re-sampling FRED maps from Klauberg *et al.* (2018).

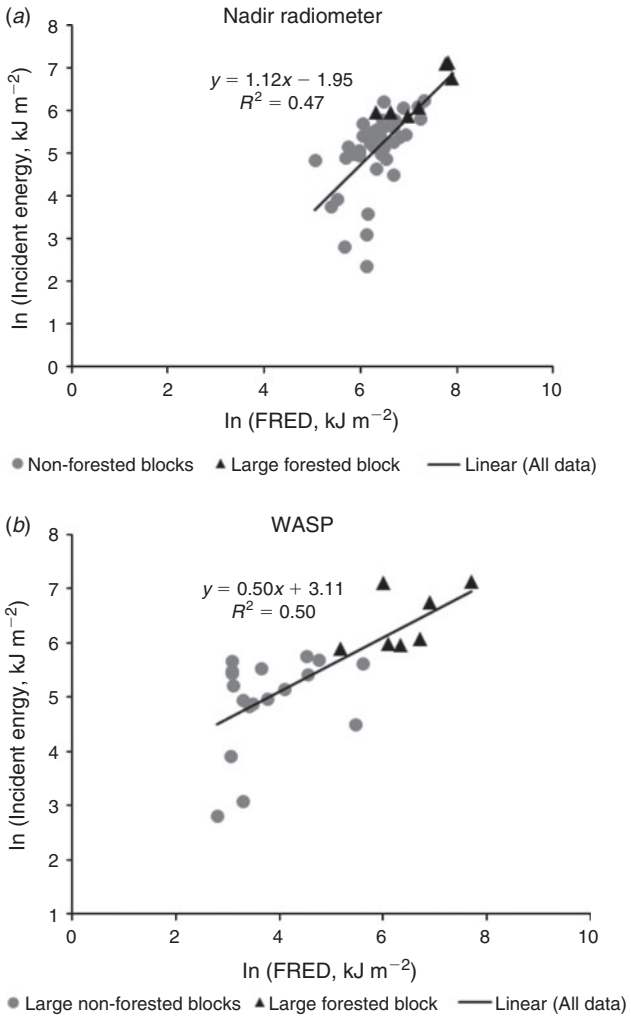

Fig. 1. Total energy (both convective and radiative) incident on *in situ* incident flux sensors as a function of remotely sensed fire radiated energy density (FRED) measured by nadir radiometers (*a*), and the Wildfire Airborne Sensor Program (WASP) longwave infrared camera (*b*). Nadir radiometers were used in all burn blocks whereas WASP measurements were only conducted for fires in large blocks. One excessively low incident energy outlier (0.26 kJ m^{-2}) from a non-forested block is excluded from the figures.

Results and discussion

Fig. 1 is a first examination of how to infer *in situ* energy deposition from spatially extensive remotely sensed active-fire measurements. The highest incident energies were in the forested block where surface-leaving radiative energy was greatest. We can also conclude that the highest incident energies were where fuel consumption was greatest as confirmed by both measurements (Hudak *et al.* 2016*b*) and the well-established correlations between FRED measured from nadir or near-nadir sensors and fuel consumption (Wooster *et al.* 2005; Freeborn *et al.* 2008; Kremens *et al.* 2012). Higher fire intensities also lead to greater incident energy (Bova and Dickinson 2005) and intensities estimated for the forested block included some of the highest in our dataset (Table 1).

Relationships between incident energy and fire characteristics, however, are not likely to be universal across fuel types and fire environments (Kremens *et al.* 2012; Frankman *et al.* 2013; Smith *et al.* 2013) and, as such, the relationships in Fig. 1 are not likely to be universal.

Uncertainty in incident energy inferred from remote measurements is particularly evident for the non-forested blocks where incident energy is plotted against FRED measurements, both log scaled to reveal bias (Fig. 1). For the five incident energy estimates with the greatest deviation from the trend lines in Fig. 1, the three for which we analysed coincident video all had flame heights below the sensor face. In future work, *in situ* sensor heights should better match expected flame heights. As well, a more physical approach to linking flame characteristics with incident energy is needed where radiative and convective heat fluxes to surfaces and objects of interest are modelled explicitly (e.g. Bova and Dickinson 2008). Apart from other benefits, a physical model could help rescale measurements to a common basis, for instance, maximum incident energy or incident energy at mid-flame height. A physical model will have to account for the often substantial variation in the partition of incident energy between convection and radiation (Frankman *et al.* 2013).

Despite interpolating FRED using primarily flame front values (Klauberg *et al.* 2018), we suspect that there remains a downward bias in WASP FRED related to temporal undersampling that would particularly affect measurements of low-energy flame fronts. The apparent bias is evident in lower estimates of FRED for WASP (Fig. 1*b*) than nadir radiometers (Fig. 1*a*). FRED measurements with high temporal frequency that include peak FRFD (such as collected by nadir radiometers) are required because the time period around the peak accounts for a large fraction of the radiation. High-spatial-resolution airborne data in Riggan *et al.* (2004) show this clearly. In relatively low-frequency airborne imagery collected from a piloted, fixed-wing aircraft that makes repeated passes over a fire, peak FRFD is only captured where image pixels coincide spatially with a flame front. If the return time is short enough relative to the residence time of the fire and the cool-down period, one can expect a reasonable estimate of time-integrated FRED for those flame-front pixels. Return intervals of 3–4 min were achieved here (Dickinson *et al.* 2016; Hudak *et al.* 2016*b*) and were ~10 min in other studies (e.g. Peterson *et al.* 2013; Schroeder *et al.* 2014). Even a 3–4-min sampling interval resulted in large parts of fire area in our non-forested burn blocks where FRED could not be estimated because of a lack of above-background FRFD measurements in time series (Klauberg *et al.* 2018). Although spatial interpolation allows continuous maps to be produced, and was used to provide data in Fig. 1, it will always be an averaged representation of fire that is dynamic in time and space (Hiers *et al.* 2009; Hoffman *et al.* 2012) and will underestimate FRED to the extent that the interpolation process includes pixels where flame-fronts were not captured. Spatial interpolation of FRED could likely be improved in future work by data-driven fire spread simulation (e.g. Rochoux *et al.* 2014, 2015).

The relationships in Fig. 1 are unlikely to be universal not only because of the likely effects of fuel and fire variability across ecosystems and temporal undersampling of fire radiation but also because of challenges for remotely sensed measurement and contrasts among remote sensors (Dickinson *et al.* 2016). We sometimes obtain non-physical estimates of the emissivity–area product (εA_f) (values >1) with the nadir radiometers that may be related to bias induced by non-ideal (i.e. non-greybody) radiation from hot gases (e.g. Dupuy *et al.* 2007; Boulet *et al.* 2009; Parent *et al.* 2010). Hot gas radiation (especially from CO_2 and CO; Boulet *et al.* 2009) is sensed because of the wide-band mid- and long-wave infrared sensors used in our nadir radiometers. A further potential source of error arises from the fact that tall flames are closer to the nadir radiometer than small flames, the effect of which could not be included in the current analysis for lack of co-located flame height measurements (see Kremens *et al.* 2010). In contrast, the WASP LWIR sensor has a narrow passband designed to avoid the influence of radiation absorption and emission by gases (Kremens and Dickinson 2015). Nadir radiometer FRED is greater than WASP FRED perhaps because it is a better estimate of total fire radiation, which includes both radiation from hot gases and greybody radiation from hot soot, fuels and substrate whereas WASP FRED may be a more accurate measurement of greybody radiation alone (Dickinson *et al.* 2016). Almost all airborne and satellite measurements in the literature likely provide better measurements of greybody than total radiation from fires (e.g. see measurements in Wooster *et al.* 2005). Differences among sensing systems in what they are measuring and measurement challenges generally (e.g. smoke absorption of radiation, Koseki and Mulholland 1991) show that we need to develop a more sophisticated understanding of wildland fire radiation and its measurement.

We now demonstrate how remotely sensed data could be used to assess woody stem mortality during surface fires. Incident energy inferred from FRED measured by nadir radiometers and WASP is used to predict depth of necrosis and, in turn, depth of necrosis is compared with bark thickness to determine threshold diameters at which turkey oak stems would survive a fire (Fig. 2). Bark thickness is whole-bark thickness, that is, depth from the bark surface to the vascular cambium, which, if killed by heating during fires around the stem's circumference, kills the stem. Note that stem death does not necessarily mean death of the entire woody plant, as many species resprout from the roots or the base of the stem. *FireStem2D* was previously used to simulate tree stem heating and stem death over a wide range of incident energy, showing a close relationship between depth of necrosis and incident energy across a range of species (Chatziefstratiou *et al.* 2013). We related modelled depth of necrosis to incident energy (E_{IT}) using a power-law fit to modelled data from fig. 7 in Chatziefstratiou *et al.* (2013). The relationship is:

$$D_N = 0.0021(E_{IT})^{0.99} \quad (3)$$

where necrosis depth (D_N) is in units of millimetres and E_{IT} in units of kilojoules per metre squared, and the relationship is limited to necrosis depths below 16 mm as appropriate for the fires in the present study. The relationship between bark thickness and turkey oak diameter is from Lutes (unpubl. data).

The median diameters of turkey oak stems that would have been expected to be killed were larger in the forested block than

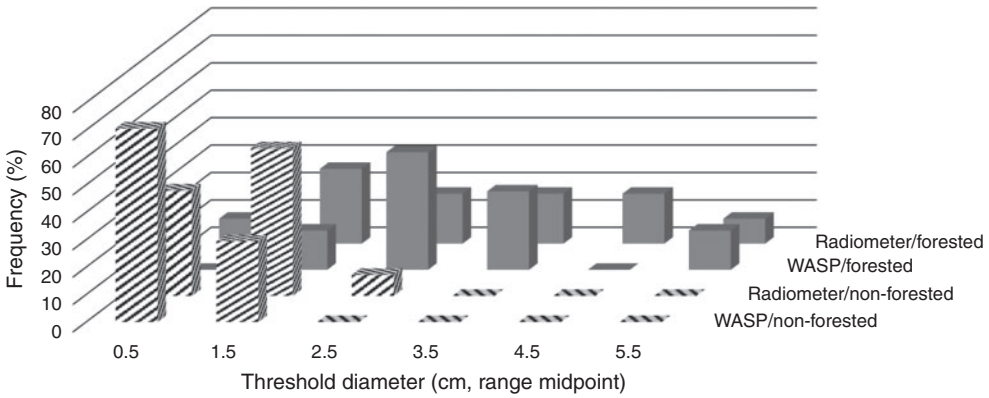

Fig. 2. Frequency distributions of threshold tree diameters in RxCADRE 2012 fires that would be vulnerable to injury during fires. Incident energy is inferred for nadir radiometer and Wildfire Airborne Sensor Program (WASP) fire radiated energy density (FRED) measurements by the relationships in Fig. 1. In turn, incident energy and modelled results from Chatziefstratiou *et al.* (2013) are used to predict necrosis depth. Finally, the diameter of the largest stem whose vascular cambium would be injured at a given incident energy (the threshold diameter) is determined from bark thickness under the assumption that injury results when necrosis depth is greater than or equal to bark thickness (i.e. cambium depth). Median threshold diameters inferred from nadir radiometer FRED are 2.6 and 1.2 cm, and from WASP FRED are 2.8 and 0.7 cm for forested and non-forested burn blocks respectively.

in the non-forested blocks (Fig. 2), consistent with the greater fuel consumption and, often, fireline intensities in forested burn blocks. Two countervailing biases may affect our predictions. We would have expected tree vulnerability to be overestimated because convective energy, and thus incident energy, is likely to be higher for the copper-plug *in situ* incident flux sensors than for tree stems. Overestimation is likely because the copper plug rapidly conducts heat away from the sensor's surface and maintains lower surface temperatures than adjacent, low-conductivity tree bark, and convection is proportional to the temperature difference between the hot flame gases and the surface to which heat is being transferred. In contrast, it appears that a handful of incident energy measurements in both forested and non-forested blocks were underestimated (see Fig. 1), probably related to small flames at some locations.

In future work, energy incident on tree stems needs to be evaluated directly in order to evaluate our stem mortality predictions. Incident energy will be affected by whether spread is backing, heading or flanking and by interactions between flames and tree stems (Gutsell and Johnson 1996). More physically realistic methods should also be explored to infer heat deposition from remotely sensed fire characteristics (Butler and Dickinson 2010). Remotely sensed flame spread, consumption and fireline intensity (e.g. Johnston *et al.* 2017) could serve as a basis for physical models of energy deposition (e.g. Bova and Dickinson 2008).

Conflicts of interest

The authors declare that they have no conflicts of interest.

Declaration of funding

The data used in this paper are from the RxCADRE 2012 campaign made possible by a grant from the Joint Fire Science Program (Project no. 11–2-1–11).

Acknowledgements

We thank the Eglin AFB fire management staff, particularly Kevin Hiers, Brett Williams and the fire crews for their high-quality work on logistics and operations. We also thank the many people whose work and collaboration made the RxCADRE project and these measurements possible, including Roger Ottmar, Dan Jimenez, Bob Kremens, Casey Teske, Paul Sopko, Mark Vosburgh and Cyle Wold, as well as the many other scientists who participated in the study. Thanks to Nick Skowronski and anonymous reviewers for feedback on earlier drafts.

References

Anderson HE (1969) Heat transfer and fire spread. USDA Forest Service, Intermountain Forest and Range Experiment Station, Research Paper INT-69. (Ogden, UT, USA)

Anderson WR, Catchpole EA, Butler BW (2010) Convective heat transfer in fire spread through fine fuel beds. *International Journal of Wildland Fire* **19**, 284–298. doi:10.1071/WF09021

Boulet P, Parent G, Collin A, Acem Z, Porterie B, Clerc JP, Consalvi JL, Kaiss A (2009) Spectral emission of flames from laboratory-scale vegetation fires. *International Journal of Wildland Fire* **18**, 875–884. doi:10.1071/WF08053

Bova AS, Dickinson MB (2005) Linking surface-fire behavior, stem heating, and tissue necrosis. *Canadian Journal of Forest Research* **35**, 814–822. doi:10.1139/X05-004

Bova AS, Dickinson MB (2008) Beyond 'fire temperatures': calibrating thermocouple probes and modeling their response to surface fires in hardwood fuels. *Canadian Journal of Forest Research* **38**, 1008–1020. doi:10.1139/X07-204

Butler BW, Dickinson MB (2010) Tree injury and mortality in fires: developing process-based models. *Fire Ecology* **6**, 55–79. doi:10.4996/FIREECOLOGY.0601055

Butler BW, Jimenez D (2009) In situ measurements of fire behavior. In '4th International fire ecology & management congress: fire as a global process, Savannah, GA', 30 November–4 December 2009, Savannah, GA, USA. (Ed. S Rideout-Hanzak) (The Association for Fire Ecology)

Butler B, Jimenez D, Forthofer J, Shannon K, Sopoko P (2010) A portable system for characterizing wildland fire behavior. In 'Proceedings of the 6th international conference on forest fire research', 15–18 November

2010, Coimbra, Portugal. (Ed. DX Viegas) [CD-ROM] (University of Coimbra: Coimbra, Portugal)

Butler BW, Teske C, Jimenez D, O'Brien JJ, Sopko P, Wold C, Vosburgh M, Hornsby B, Loudermilk EL (2016) Observations of energy transport and rate of spreads from low-intensity fires in longleaf pine habitat – RxCADRE 2012. *International Journal of Wildland Fire* **25**, 76–89. doi:10.1071/WF14154

Cannon JB, O'Brien JJ, Loudermilk EL, Dickinson MB, Peterson CJ (2014) The influence of experimental wind disturbance on forest fuels and fire characteristics. *Forest Ecology and Management* **330**, 294–303. doi:10.1016/J.FORECO.2014.07.021

Chatziefstratiou EK, Bohrer G, Bova AS, Subramanian R, Frasson RPM, Scherzer A, Butler BW, Dickinson MB (2013) FireStem2D – A two-dimensional heat transfer model for simulating tree stem injury in fires. *PLoS One* **8**(7), e70110. doi:10.1371/JOURNAL.PONE.0070110

Dickinson MB, Kremens R (2015) RxCADRE 2008, 2011, and 2012: radiometer data. USFS Forest Service Research Data Archive. (Fort Collins, CO, USA)

Dickinson MB, Ryan KC (2010) Introduction: strengthening the foundation of wildland fire effects prediction for research and management. *Fire Ecology* **6**, 1–12. doi:10.4996/FIREECOLOGY.0601001

Dickinson MB, Hudak AT, Zajkowski T, Loudermilk EL, Schroeder W, Ellison L, Kremens RL, Holley W, Martinez O, Paxton A (2016) Measuring radiant emissions from entire prescribed fires with ground, airborne and satellite sensors - RxCADRE 2012. *International Journal of Wildland Fire* **25**, 48–61. doi:10.1071/WF15090

Dupuy JL, Vachet P, Maréchal J, Meléndez J, de Castro AJ (2007) Thermal infrared emission–transmission measurements in flames from a cylindrical forest fuel burner. *International Journal of Wildland Fire* **16**, 324–340. doi:10.1071/WF06043

Finney MA, Cohen JD, Grenfell IC, Yedinak KM (2010) An examination of fire spread thresholds in discontinuous fuel beds. *International Journal of Wildland Fire* **19**, 163–170. doi:10.1071/WF07177

Finney MA, Cohen JD, Forthofer JM, McAllister SS, Gollner MJ, Gorham DJ, Saito K, Akafuah NK, Adam BA, English JD (2015) Role of buoyant flame dynamics in wildfire spread. *Proceedings of the National Academy of Sciences of the United States of America* **112**, 9833–9838. doi:10.1073/PNAS.1504498112

Frankman D, Webb BW, Butler BW, Jimenez D, Forthofer JM, Sopko P, Shannon KS, Hiers JK, Ottmar RD (2013) Measurements of convective and radiative heating in wildland fires. *International Journal of Wildland Fire* **22**, 157–167. doi:10.1071/WF11097

Freeborn PH, Wooster MJ, Hao WM, Ryan CA, Nordgren BL, Baker SP, Ichoku C (2008) Relationships between energy release, fuel mass loss, and trace gas and aerosol emissions during laboratory biomass fires. *Journal of Geophysical Research* **113**, D01301. doi:10.1029/2007JD008679

Giglio L, Van Der Werf GR, Randerson JT, Collatz GJ, Kasibhatla P (2006) Global estimation of burned area using MODIS active fire observations. *Atmospheric Chemistry and Physics* **6**, 957–974. doi:10.5194/ACP-6-957-2006

Gutsell SL, Johnson EA (1996) How fire scars are formed: coupling a disturbance process to its ecological effect. *Canadian Journal of Forest Research* **26**, 166–174. doi:10.1139/X26-020

Hiers JK, O'Brien JJ, Mitchell RJ, Grego JM, Loudermilk EL (2009) The wildland fuel cell concept: an approach to characterize fine-scale variation in fuels and fire in frequently burned longleaf pine forests. *International Journal of Wildland Fire* **18**, 315–325. doi:10.1071/WF08084

Hoffman C, Morgan P, Mell W, Parsons R, Strand EK, Cook S (2012) Numerical simulation of crown fire hazard immediately after bark beetle-caused mortality in lodgepole pine forests. *Forest Science* **58**, 178–188. doi:10.5849/FORSCI.10-137

Hudak A, Bright BC, Kremens R, Dickinson MB (2016*a*) Wildfire Airborne Sensor Program orthorectified and calibrated long-wave infrared images. USDA Forest Service. (Fort Collins, CO, USA)

Hudak AT, Dickinson MB, Bright BC, Kremens RL, Loudermilk EL, O'Brien JJ, Hornsby BS, Ottmar RD (2016*b*) Measurements relating fire radiative energy density and surface fuel consumption – RxCADRE 2011 and 2012. *International Journal of Wildland Fire* **25**, 25–37. doi:10.1071/WF14159

Ichoku C, Kaufman YJ (2005) A method to derive smoke emission rates from MODIS fire radiative energy measurements. *IEEE Transactions on Geoscience and Remote Sensing* **43**, 2636–2649. doi:10.1109/TGRS.2005.857328

Johnston JM, Wooster MJ, Paugam R, Wang X, Lynham TJ, Johnston LM (2017) Direct estimation of Byram's fire intensity from infrared remote sensing imagery. *International Journal of Wildland Fire* **26**, 668–684. doi:10.1071/WF16178

Klauberg C, Hudak AT, Bright BC, Boschetti L, Dickinson MB, Kremens RL, Silva CA (2018) Use of ordinary kriging and Gaussian conditional simulation to interpolate airborne fire radiative energy density estimates. *International Journal of Wildland Fire* **27**, 228–240. doi:10.1071/WF17113

Koseki H, Mulholland GW (1991) The effect of diameter on the burning of crude oil fires. *Fire Technology* **27**, 54–65. doi:10.1007/BF01039527

Kremens RL, Dickinson MB (2015) Estimating radiated flux density from wildland fires using the raw output of limited bandpass detectors. *International Journal of Wildland Fire* **24**, 461–469. doi:10.1071/WF14036

Kremens RL, Smith AMS, Dickinson MB (2010) Fire metrology: current and future directions in physics-based measurements. *Fire Ecology* **6**, 13–25. doi:10.4996/FIREECOLOGY.0602013

Kremens R, Dickinson M, Bova A (2012) Radiant flux density, energy density and fuel consumption in mixed-oak forest surface fires. *International Journal of Wildland Fire* **21**, 722–730. doi:10.1071/WF10143

Lentile LB, Holden ZA, Smith AMS, Falkowski MJ, Hudak AT, Morgan P, Lewis SA, Gessler PE, Benson NC (2006) Remote sensing techniques to assess active fire characteristics and post-fire effects. *International Journal of Wildland Fire* **15**, 319–345. doi:10.1071/WF05097

Massman WJ (2015) A non-equilibrium model for soil heating and moisture transport during extreme surface heating. *Geoscientific Model Development* **8**, 3659–3680. doi:10.5194/GMD-8-3659-2015

Ottmar RD, Hiers JK, Butler BW, Clements CB, Dickinson MB, Hudak AT, O'Brien JJ, Potter BE, Rowell EM, Strand TM (2016*a*) Measurements, datasets and preliminary results from the RxCADRE project – 2008, 2011 and 2012. *International Journal of Wildland Fire* **25**, 1–9. doi:10.1071/WF14161

Ottmar RD, Hudak AT, Prichard SJ, Wright CS, Restaino JC, Kennedy MC, Vihnanek RE (2016*b*) Pre-fire and post-fire surface fuel and cover measurements collected in the south-eastern United States for model evaluation and development – RxCADRE 2008, 2011 and 2012. *International Journal of Wildland Fire* **25**, 10–24. doi:10.1071/WF15092

Parent G, Acem Z, Lechêne S, Boulet P (2010) Measurement of infrared radiation emitted by the flame of a vegetation fire. *International Journal of Thermal Sciences* **49**, 555–562. doi:10.1016/J.IJTHERMALSCI.2009.08.006

Paugam R, Wooster MJ, Roberts G (2013) Use of handheld thermal imager data for airborne mapping of fire radiative power and energy and flame front rate of spread. *IEEE Transactions on Geoscience and Remote Sensing* **51**, 3385–3399. doi:10.1109/TGRS.2012.2220368

Peterson D, Wang J, Ichoku C, Hyer E, Ambrosia V (2013) A sub-pixel-based calculation of fire radiative power from MODIS observations. 1: Algorithm development and initial assessment. *Remote Sensing of Environment* **129**, 262–279. doi:10.1016/J.RSE.2012.10.036

Riggan PJ, Tissell RG, Lockwood RN, Brass JA, Pereira JAR, Miranda HS, Miranda AC, Campos T, Higgins R (2004) Remote measurement of energy and carbon flux from wildfires in Brazil. *Ecological Applications* **14**, 855–872. doi:10.1890/02-5162

Rochoux MC, Ricci S, Lucor D, Cuenot B, Trouvé A (2014) Towards predictive data-driven simulations of wildfire spread – Part I: Reduced-cost

ensemble Kalman filter based on a polynomial chaos surrogate model for parameter estimation. *Natural Hazards and Earth System Sciences* **14**, 2951–2973. doi:10.5194/NHESS-14-2951-2014

Rochoux MC, Emery C, Ricci S, Cuenot B, Trouvé A (2015) Towards predictive data-driven simulations of wildfire spread – Part II: Ensemble Kalman filter for the state estimation of a front-tracking simulator of wildfire spread. *Natural Hazards and Earth System Sciences* **15**, 1721–1739. doi:10.5194/NHESS-15-1721-2015

Sacadura JF (2005) Radiative heat transfer in fire safety science. *Journal of Quantitative Spectroscopy & Radiative Transfer* **93**, 5–24. doi:10.1016/J.JQSRT.2004.08.011

Schroeder W, Ellicott E, Ichoku C, Ellison L, Dickinson MB, Ottmar RD, Clements C, Hall D, Ambrosia V, Kremens RL (2014) Integrated active fire retrievals and biomass burning emissions using complementary near-coincident ground, airborne and spaceborne sensor data. *Remote Sensing of Environment* **140**, 719–730. doi:10.1016/J.RSE.2013.10.010

Smith A, Tinkham WT, Roy DP, Boschetti L, Kremens RL, Kumar SS, Sparks AM, Falkowski MJ (2013) Quantification of fuel moisture effects on biomass consumed derived from fire radiative energy retrievals. *Geophysical Research Letters* **40**, 6298–6302. doi:10.1002/2013GL058232

Viskanta R (2008) Overview of some radiative transfer issues in simulation of unwanted fires. *International Journal of Thermal Sciences* **47**, 1563–1570. doi:10.1016/J.IJTHERMALSCI.2008.01.008

Wooster MJ, Zhukov B, Oertel D (2003) Fire radiative energy for quantitative study of biomass burning: derivation from the BIRD experimental satellite and comparison to MODIS fire products. *Remote Sensing of Environment* **86**, 83–107. doi:10.1016/S0034-4257(03)00070-1

Wooster MJ, Roberts G, Perry GLW, Kaufman YJ (2005) Retrieval of biomass combustion rates and totals from fire radiative power observations: FRP derivation and calibration relationships between biomass consumption and fire radiative energy release. *Journal of Geophysical Research, D, Atmospheres* **110**, D24311. doi:10.1029/2005JD006318

Yedinak KM, Forthofer JM, Cohen JD, Finney MA (2006) Analysis of the profile of an open flame from a vertical fuel source. *Forest Ecology and Management* **234**, S89.